The Journal of Experimental Biology 209, 3001-3017
Published by The Company of Biologists 2006
doi:10.1242/jeb.02305

Free-flight responses of *Drosophila melanogaster* to attractive odors

Seth A. Budick[1,*] and Michael H. Dickinson[1,2]

[1]*Division of Biology and* [2]*Bioengineering Option, California Institute of Technology, Pasadena, CA 91125, USA*

*Author for correspondence (e-mail: sbudick@caltech.edu)

Accepted 26 April 2006

Summary

Many motile organisms localize the source of attractive odorants by following plumes upwind. In the case of *D. melanogaster*, little is known of how individuals alter their flight trajectories after encountering and losing a plume of an attractive odorant. We have characterized the three-dimensional flight behavior of *D. melanogaster* in a wind tunnel under a variety of odor conditions. In the absence of olfactory cues, hungry flies initiate flight and display anemotactic orientation. Following contact with a narrow ribbon plume of an attractive odor, flies reduce their crosswind velocity while flying faster upwind, resulting in a surge directed toward the odor source. Following loss of odor contact due to plume truncation, flies frequently initiate a stereotyped crosswind casting response, a behavior rarely observed in a continuous odor plume. Similarly, within a homogeneous odor cloud, flies move fast while maintaining an upwind heading. These results indicate both similarities and differences between the behavior of *D. melanogaster* and the responses of male moths to pheromone plumes, suggesting possible differences in underlying neural mechanisms.

Key words: *Drosophila*, insect, free flight, odor, olfaction, search, chemotaxis, anemotaxis, flight control.

Introduction

The responses of flying insects to attractive odors have fascinated biologists since Fabre's time and have served as a model system in neuroethology for decades (see Cardé and Minks, 1997). Kennedy first showed that mosquitoes flying upwind rely on motion of the visual world to control their ground speed (Kennedy, 1940), a mechanism referred to as 'optomotor anemotaxis'. Kennedy and Marsh later extended this finding to male moths flying up a pheromone plume (Kennedy and Marsh, 1974), and also observed that moths do not always fly directly upwind, but instead make iterated zigzagging counterturns biased in the upwind direction (Marsh et al., 1978). The temporal regularity of these counterturns is also a feature of casting, a behavior that typically follows plume loss or entry into a homogenous plume, and which is characterized by repeated turns, interspersed with wide lateral excursions roughly perpendicular to the wind-line (Kennedy et al., 1980; Kennedy et al., 1981). These observations led to the hypothesis that these turns are generated by an internal pattern generator that is modulated by plume characteristics such as odor concentration (Kennedy, 1983; Kuenen and Baker, 1983).

More recently, researchers have placed increased emphasis on the importance of the temporal structure of olfactory stimuli in maintaining upwind flight (Baker et al., 1985). Baker and Haynes (Baker and Haynes, 1987) demonstrated that at least one species of moth is capable of responding rapidly to individual episodes of plume contact and loss while following a shifting plume. Baker (Baker, 1990) used this result and related neurophysiological data to formulate a model for the neural mechanisms mediating the odor response. He postulated that there is a phasically modulated response that generates an upwind surge on plume contact, but which decays rapidly due to adaptation. There is also a separate tonic response that activates an internal counterturn generating program, but which can be inhibited by the phasic response. In a pulsed odor plume, the arrival of odor packets at the appropriate frequency could prevent adaptation of the phasic response while maintaining the suppression of the tonic pathway, yielding a trajectory that resembles a fused series of upwind surges. This model neatly explains a variety of prior data and has gained support from experiments involving pulsed plumes in two species of moths (Mafra-Neto and Cardé, 1994; Vickers and Baker, 1994), but its relevance to flight in other insect orders has not been widely tested.

The fact that odor-modulated locomotion seems to be highly stereotypical in a variety of species may suggest that this method of odor tracking has a strong selective advantage that transcends taxonomic boundaries, though it could also reflect a constraint based on shared ancestry. For this reason, it is especially useful to examine olfactory localization in species outside the Lepidoptera. Odor-modulated, and indeed upwind flight generally, has been relatively little studied in *Drosophila* despite its importance as a general model system for genetics, behavior and physiology (David, 1979a; David, 1979b; David,

1982; Kellogg et al., 1962; Wright, 1964). Anecdotal reports have suggested that the flight behavior of *D. melanogaster* may differ substantially from that reported for moths in that sustained upwind flight does not seem to require intermittent stimulation (Wright, 1964). Recent work in a mosquito (*Aedes aegypti*) has also indicated that intermittent stimulation is not necessarily a universal prerequisite for upwind flight (Geier et al., 1999).

In this study, we have characterized the changes in the flight trajectories of *D. melanogaster* in ribbon and large diameter odor plumes and in a homogeneous odor cloud presented within a wind tunnel. Although a description of the envelope of wind conditions under which *D. melanogaster* actually localize odor plumes in the wild is unavailable, it seems likely that much odor localization occurs in air moving at moderate velocities, where turbulent rather than molecular diffusion dominates transport, making these results germane to behavior in the natural world. Our data indicate that *D. melanogaster* share several features of odor-modulated flight with well-studied Lepidopteran species. Nevertheless, fruit flies seem to differ in several important ways, not least of which is the persistence of straight upwind flight in the presence of a homogeneous odor cloud. These results may require modification of the phasic/tonic model of odor-mediated flight in order to make it more generally applicable to *D. melanogaster* and other species.

Materials and methods

Wind tunnel

An open circuit, closed throat wind tunnel was built commercially to custom specifications (Engineering Laboratory Design, Inc., Lake City, MN, USA). At the intake end, air was drawn through a honeycomb and screen pack followed by a 6.25:1 contraction and then a 1.55 m long working section, constructed from acrylic, with a width and height of 0.305 m (Fig. 1A). The working section was followed by a diffuser and then the fan. At the upwind and downwind ends of the working section, 1 mm mesh prevented the flies from escaping from the tunnel. All ducts were fabricated from fiberglass reinforced plastic.

The floor of the tunnel was painted black with acrylic paint to aid in fly visualization as described below. The walls of the tunnel were covered by a random pattern consisting of black and white squares of length 1.4 cm. At this size, a square normal to the fly would subtend 5° of visual space when viewed from the midline of the tunnel. The checkerboard patterns were perforated at half their height to allow for illumination *via* infrared diodes positioned outside the tunnel, again to aid in fly visualization.

In experiments utilizing wind, the velocity was set to 0.4 m s^{-1}. This value was selected because odor source localization was robust at that speed while being inhibited at higher velocities. Furthermore, our own observations of wind velocities in an orange orchard in which *Drosophila* spp. were active indicated that this value was well within the normal range of variation both beneath individual orange trees and in the open spaces between trees (mean velocity 0.37±0.35 m s^{-1}).

Summary of experiments

In experiment 1, flies were flown (a) in the absence of wind and odor, or (b) in the presence of wind but in the absence of odor. In experiment 2, flies were flown with a conspicuous visual object (a black post, 1.27 cm in diameter and spanning the height of the working section, positioned at a point halfway along the long axis of the tunnel, 6.35 cm from the nearest wall) either (a) in the absence of wind and odor, or (b) in the presence of wind but in the absence of odor. In experiment 3, flies were flown either (a) in the presence of a banana odor ribbon plume, or (b) in a no odor control with a clean air ribbon plume. In experiment 4, flies were flown (a) in the presence of wind but in the absence of odor, or (b) in the presence of wind and a homogeneous banana odor cloud. In the final experiment (5), flies were flown (a) in a pulsed or (b) a continuous, large-diameter banana odor plume, or (c) in a pulsed no odor control. In all experiments, flies were restricted to one treatment per day to avoid odor contamination.

Odor

Banana odor was produced by macerating ripe banana, together with distilled H_2O and baker's yeast, in the ratio 1 g banana:1 ml H_2O:0.02 g yeast. This recipe was chosen on the basis of its demonstrated ability to lure wild flies to outdoor traps and is derived from standard *Drosophila* bait recipes (e.g. Carson and Heed, 1986). This mixture was allowed to ferment for 45 min at 25°C and was then filtered through 0.1 mm mesh for an additional hour. The filtrate was produced in quantities of 0.5–1 l and frozen immediately for later use.

Fly responses were tested in three differently structured odor plumes. In ribbon plume experiments, air was bubbled through the banana mixture at a rate of 0.3 l min^{-1} by means of a volume flow controller (Sierra Side Trak, Monterey, CA, USA). The banana mixture was contained within a polypropylene vial with clean air passing into the vial *via* a 3·mm diameter brass tube that penetrated the vial's lid. The tube descended slightly less than the height of the vial such that the air emerging from it bubbled through 50 ml of the banana mixture. The scented air then passed out of the vial *via* a PVC tube attached to the vial's lid and passed into an acrylic tube of 3 mm diameter that penetrated the tunnel floor 13 cm from the upwind end of the working section, halfway between the two tunnel walls. This acrylic tube was bent 90° at a height of 15.25 cm, half the height of the tunnel, and a polypropylene nozzle, diameter 2 mm, was glued to the end of the tube. In wide plume experiments, the scented air was injected into the banana mixture at 1.0 l min^{-1} and passed down a 3 mm diameter brass tube that penetrated the tunnel floor in the same position as in the ribbon plume experiments. This brass tube was then inserted in, and glued to, the end of a 7 mm diameter acrylic tube, 157 mm in length, parallel to the tunnel floor. This tube was perforated by a 1 mm diameter hole at its downwind

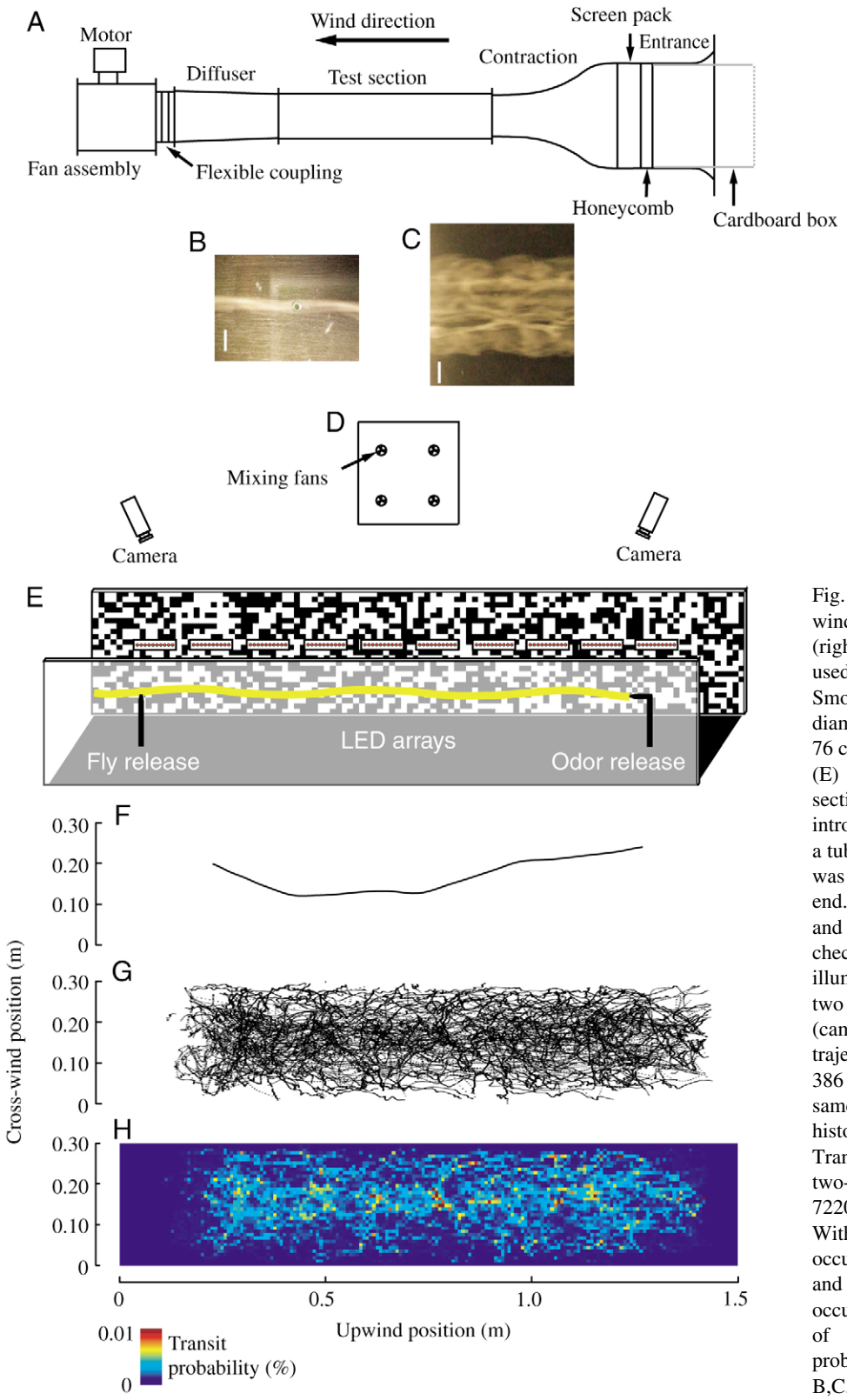

Fig. 1. (A) Schematic profile view of the full wind tunnel. Gray/dotted line at upwind end (right) represents the 76 cm cardboard box used for generation of the homogeneous cloud. Smoke visualization of the ribbon (B) and large diameter (C) plumes. (D) Front view of the 76 cm cardboard box with four mixing fans. (E) Schematic representation of the working section of the wind tunnel. Flies were introduced *via* a pipette tip glued to the end of a tube at the downwind end of the tunnel; odor was introduced *via* a second tube at the upwind end. The floor of the tunnel was painted black and the walls were covered with a random checkerboard pattern. Arrays of IR diodes illuminated the tunnel, which was visualized by two IR-sensitive cameras positioned above it (camera positions not to scale). (F) A sample trajectory in a no odor, control treatment. (G) 386 overlaid trajectory fragments from the same treatment. (H) A transit probability histogram derived from the trajectories in G. Transit histograms were derived by dividing two-dimensional views of the wind tunnel into 7220 squares with side lengths of 0.8 cm. Within a given treatment, the number of fly occurrences within each square was summed and divided by the total number of fly occurrences in all squares to yield a probability of square occupancy, where the total probability summed to 1.0. Scale bars: 1 cm in B,C.

end and three additional sets of four concentric holes, with one set each at 5, 10 and 15 cm along its length. Due to the pressure differential along the length of this tube, gas exiting the more proximal holes was projected further from the tube, resulting in a diffuse cylindrical plume. The wide plume was either produced continuously, or was pulsed via a three-way solenoid valve (Valve Driver II, General Valve Corp., Fairfield, NJ, USA) controlled by custom software running on a PC. This

valve was downstream of the flow controller and switched a clean air input between one output that led to the vial containing the banana odor and a second output, which simply consisted of a PVC tube. Those two output lines were then reunited *via* a Y junction just prior to reaching the brass tube that passed through the tunnel floor, thus switching the odor and clean air inputs to the tunnel. In the pulsed plume, the banana odor alternated with clean air at 1 s intervals. By switching the input to clean air, the odor was evacuated very rapidly from the tube following the truncation of each pulse, producing very sharp boundaries at both the leading and lagging edges of the pulse, as judged from smoke visualization.

To visualize the odor plume produced by these delivery systems, we generated a smoke plume by pumping mineral oil through a hypodermic needle, across which we placed a high voltage that burned the oil. The smoke thus generated was then injected into the tunnel under the same conditions as in the odor plume experiments and the plume's trajectory and dimensions were measured. The ribbon plume was slightly sinuous, with a mean instantaneous diameter of 0.68±0.09 cm, measured at 10 points spaced 1 cm apart along its length (Fig. 1B). The envelope described by the undulating plume, along this same length, was 1.01 cm and thus for analytical purposes, we modeled the plume as a 1 cm diameter cylinder. We similarly measured the mean instantaneous diameter of the large diameter plume as 4.84±0.24 cm and this plume was thus modeled as a 4.84 cm diameter cylinder (Fig. 1C). The position of the plume within the tunnel was determined by recording its position at its upwind entrance and at the downwind exit and linearly interpolating between the two.

Homogeneous odor cloud experiments used the same banana odor, but in this case, air was pumped into 100 ml of the filtrate at 25.5 l min^{-1}. A large cardboard box, 76 cm square, was inserted into the tunnel inlet and served as a mixing chamber for the odor. Four computer fans were positioned approximately equidistant from each other and from the walls of the cardboard box (Fig. 1D). Four PVC tubes carried the odor from the vial to the cardboard box where the odor was released immediately upstream of the four small fans and was mixed thoroughly in the mixing chamber (as judged by experiments with smoke tracers). By the time it reached the working section, however, the smoke plume was too diffuse to visualize. Normalizing the odor density of the ribbon plume to 100%, the calculated densities of the wide plume and homogeneous cloud were 18% and 11%, respectively.

Animals

Experiments were performed at 25°C on 3- to 5-day-old female fruit flies, *Drosophila melanogaster* Meigen, descended from a wild-caught population of 200 mated females. Animals were deprived of food, but not water, for 20–24 h prior to experimentation in order to motivate flight. On the day of experimentation, approximately 100 flies were kept in a 50 ml vial beneath the tunnel where they acclimated for 10 min to 2 h, depending on when they were introduced into the tunnel, as described below, with an experiment lasting approximately 2 h. This vial was connected, *via* a stop cock, to an acrylic tube of diameter 5 mm that penetrated the floor of the tunnel at a distance 16.7 cm from the downwind end of the working section. This tube was capped by a pipette tip such that flies emerging from the tube were positioned halfway between the tunnel walls and at approximately half the height of the tunnel. Flies were introduced into the tunnel individually such that the odor plume intercepted the fly release tube at approximately the height of the emerging flies, immediately exposing them to the odor. If a fly did not take flight shortly after emerging into the tunnel, one or more flies were introduced in order to increase the probability that one would do so. Flies were captured by the imaging system from take-off at the release tube or shortly after take-off. Individual trajectories were often recorded as several trajectory fragments due to loss of the fly by the visualization system. As such, a single mean value based on all trajectory fragments was calculated for each trajectory parameter for each fly, except as noted below. In all experiments, flies were recorded until they landed. The flies were vacuumed out of the tunnel approximately every 10 min.

Tunnel illumination and fly visualization

The tunnel was illuminated by a linear array of 10 halogen bulbs on each side yielding a luminance of 60–120 lux within the working section. IR LEDs (HSDL-4200, Hewlett Packard, Palo Alto, CA, USA) positioned at the mid-height of the tunnel provided illumination for two near IR sensitive cameras (SSC-M350, Sony, Tokyo, Japan) positioned 1.27 m above the tunnel at a distance of 1.82 m from each other (Fig. 1E). The 3-dimensional (3-D) flight trajectories were sampled at 60 frames s^{-1} and reconstructed with commercially available software, Trackit 3-D (Fry et al., 2000). In the pulsed plume experiments, the state of the solenoid valve was recorded at every time point together with the 3-D fly position. We were thus able to determine the location of all pulses in the tunnel at any given time as well as the fly's position relative to them. This allowed us to determine the moment of plume entry and plume loss. The fly trajectories were smoothed to remove digitization errors by low-pass filtering with a fifth order Butterworth filter using a frequency cut-off of 7.5 Hz.

All analyses of fly trajectories made use of software written using Matlab (Mathworks). Only trajectories longer than 0.42 s were analyzed in order to be of sufficient length for low pass filtering. Flies approaching the odor source generally slowed down and ceased to respond with upwind surges, due either to the visual effects of the plume source, changes in plume dynamics, or both. Because of these qualitative changes in flight trajectories as the animals approached and landed on the odor release site, flight within the most upwind 0.25 m of the tunnel was excluded from quantitative analyses. In order to visualize the distribution of flies within the wind tunnel, individual trajectories (Fig. 1F) were overlaid (Fig. 1G), and plotted as pseudocolor transit probability histograms (Fig. 1H). Flight trajectories were described in terms of a number of variables that were calculated at every frame in the flight trajectory (Fig. 2). Ground speed was determined from

the distance that the animal traveled in the horizontal plane between samples. Cross-wind velocity and upwind velocity were the components of ground speed directed across the width of the tunnel and up its long axis, respectively. Vertical velocity was determined from the distance that the animal traveled in the vertical plane between samples. 3-D heading was the angle formed by the tangent to the flight trajectory and the long axis of the tunnel, such that 0° corresponded to straight upwind and 180° was straight downwind. 3-D heading is thus intentionally underdefined in that a value of 90° could correspond to any vector within the transverse vertical plane of the fly. Heading (track angle) was the projection of 3-D heading in the horizontal plane of the fly and is equivalent to the angle between the ground speed vector and the long axis of the tunnel. Airspeed was calculated trigonometrically using ground speed, wind speed and heading, and is the velocity of the animal in the horizontal plane relative to the wind. Finally, plume distance was defined as the shortest absolute 3-D distance between the fly and the plume. Substantial variability in the overall shape of flight trajectories, relative to published trajectories for moths, made it difficult to assign meaningful parameters to the counterturning behavior, such as turn frequency or inter-reversal distance.

Statistical analysis

All linearly distributed trajectory parameters were compared using heteroscedastic *t*-tests whereas count data were compared with χ^2 tests. Heading data were circularly distributed and thus required treatment with the appropriate statistical methods. For each trajectory, a mean heading was calculated by treating the instantaneous heading between each pair of frames as a unit vector with angle θ_i. The rectangular components of this unit vector are then: $C_i=\cos\theta_i$ and $S_i=\sin\theta_i$. Summing over the entire trajectory and dividing by trajectory length yields the rectangular coordinates of the mean vector:

$$\bar{C} = \frac{1}{n}\sum_{i=1}^{n} C_i\,, \qquad \bar{S} = \frac{1}{n}\sum_{i=1}^{n} S_i\,.$$

The angle of the mean vector, $\bar{\theta}$, is then calculated as:

$$\bar{\theta} = \begin{cases} \tan^{-1}(\bar{S}/\bar{C}) & \text{if} \quad \bar{C}>0 \\ \tan^{-1}(\bar{S}/\bar{C})+180° & \text{if} \quad \bar{C}<0 \\ 90° & \text{if} \quad \bar{C}=0 \quad \text{and} \quad \bar{S}>0 \\ 270° & \text{if} \quad \bar{C}=0 \quad \text{and} \quad \bar{S}<0 \end{cases} .$$

The length of the mean vector, r, is calculated as $r=[\bar{C}^2+\bar{S}^2]^{\frac{1}{2}}$. This value varies between 0 and 1 and is a measure of the dispersion around the mean heading (Batschelet, 1981). The mean angular deviation, a quantity equivalent to the standard deviation in linear statistics, is then defined as $s=[2(1-r)]^{\frac{1}{2}}$. Circular means are thus reported here as mean ± s while means of linear parameters are reported with the standard deviation (s.d.).

To test for differences in mean direction between

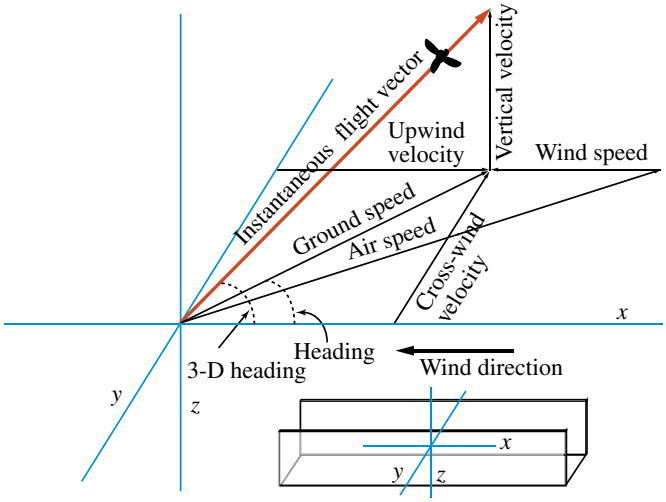

Fig. 2. Trajectory parameters subjected to analysis (explanations in text).

experimental conditions, we implemented the non-parametric test for common mean direction suggested by Fisher [(Fisher, 1993), pp. 115–117]. To test for differences in the angular dispersions of two samples about their respective means, we used the non-parametric test suggested by Batschelet [(Batschelet, 1981), pp. 124–126]. Non-parametric tests were used due to their limited assumptions about angular distributions, namely that the data need not be fit by von Mises distributions.

In several cases, mean trajectory headings did not appear to be unimodally distributed so we tested the fit of one or more von Mises distributions using the method of moments [(Fisher, 1993), pp. 100–102]. A von Mises distribution is described by two parameters, μ and κ. For a given distribution, the maximum likelihood estimate of μ is $\bar{\theta}$ while κ is estimated as the solution of the equation: $A_1(\kappa)=r$, where $A_1(x)=I_1(x)/I_0(x)$, the ratio of two modified Bessel functions. We begin by fitting a single von Mises distribution (1VM) to a sample of mean heading vectors, estimating μ and κ and testing the goodness of fit (*gof*) of a unimodal model. The goodness of fit statistic U^2 is calculated as:

$$U^2 = \left\{\sum_{i=1}^{n} [z_i - (2i-1)/2n]^2\right\} - n(\bar{z}-\tfrac{1}{2}) + (1/12n)\,,$$

where n is the sample size and the z_i are the cumulative frequency values of the individual mean trajectory headings rearranged into ascending order. In successive iterations, we fit a model containing one additional mode (2VM, etc.), and estimate the values of μ and κ for each mode and the proportion of the total sample represented by each. The *gof* of the new model is calculated to obtain U^2_{VM}. To assess the significance probability of the fit, we generate 100 parametric bootstrap samples of the same size as the original dataset. For each sample, we estimate μ and κ and calculate the corresponding *gof*. The significance probability of the fit (P_{VM})

is then estimated as $P_{VM}=N_{U_2}/100$, where N_{U_2} is the number of bootstrap samples for which the *gof* exceeds U^2_{VM}. All statistical analyses were conducted using custom routines written in Matlab.

Results

Experiment 1: Anemotaxis

While flying in the wind tunnel, *D. melanogaster* were anemotactic (Fig. 3A–D). In the absence of both odor and wind, flies tended to remain in the 'downwind' portion of the tunnel (Fig. 3A), whereas in a 0.4 m s^{-1} wind with no odor, flies were distributed relatively uniformly along the tunnel's length (Fig. 3B). Furthermore, mean trajectory headings seemed to be directed bimodally along the longitudinal axis of the tunnel in still air (Fig. 3C), but unimodally upwind in the presence of wind (Fig. 3D). We tested both unimodal and bimodal fits of von Mises distributions to the mean trajectories both in the presence and absence of wind (Tables 1 and 2). In both cases, a model containing two modes was a better fit to the data than was a unimodal model. Comparing those bimodal fits, however, in still air, the mode directed towards –2.91±28.30° (approximately upwind), accounted for only 58% of the data (Table 1) while with wind present, the mode directed towards 1.46±13.67° captured 93% of the sample (Table 2). Thus, while both samples were better fit by bimodal distributions, the mode representing upwind flight was substantially larger in the presence of wind. The distribution of mean trajectory headings around approximately 0° and 180° in still air indicates that wind did not simply increase activity levels, but actually affected flight headings. Furthermore, non-parametric circular tests indicated no significant differences between the mean headings (d.f.=1, Y_2=0.025, P=0.87) although the dispersions around the two respective mean headings did differ significantly (N=80, U=2730, P<0.0001). While flying

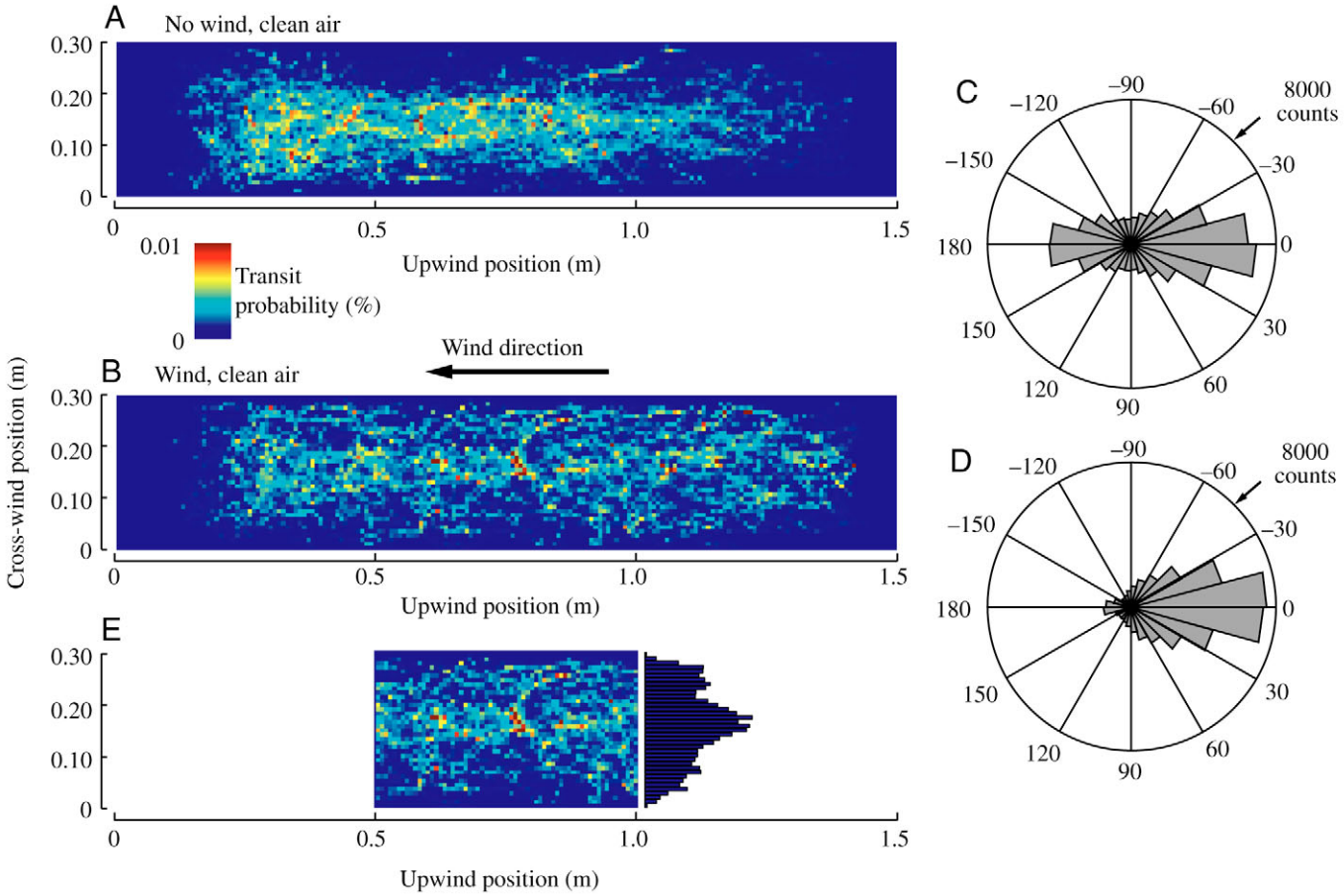

Fig. 3. *D. melanogaster* are anemotactic and manifest a centering response. Transit histograms, viewed from above, of flies released at the downstream end of the tunnel in still air (A, 132 flies) and in the presence of a 0.4 m s^{-1} wind (B, 80 flies). Based on a mixture of von Mises distributions, flight headings were bimodally distributed up (–2.91±28.30°) and down (177.72±32.45°) the longitudinal axis of the tunnel in still air (C), but were unimodally centered on 1.46±13.67° in the presence of wind (D). Raw counts of instantaneous heading values are plotted in C and D, but all statistical analyses are on mean trajectory headings, which were significantly more dispersed in the absence of wind (N=80, U=2730, P<0.0001). (E) A histogram of the distribution of flies across the tunnel's width indicates that flies manifested a centering response within the central 0.5 m of the tunnel in a 0.4 m s^{-1} wind. Flight in only the central section was analyzed in order to minimize the visual effects of the odor- and fly-releasing tubes.

Table 1. *Fitting a mixture of von Mises distributions to mean heading vectors of flies in a no odor, no wind environment*

Model	*gof* (U^2)	*P*	μ_1 (degrees)	*s* (degrees)	p_1	μ_2 (degrees)	*s* (degrees)	p_2
1VM	0.644	<0.01	1.26±178.37	74.51	1.00	–	–	–
2VM	0.098	0.16	–2.91±6.55	28.30	0.58	177.72±8.83	32.45	0.42

For each model, a goodness of fit was calculated and significance tested against a parametric bootstrap as described in the Materials and methods. The mean direction of each mode (μ±95%CI) as well as the angular standard deviation (*s*) and proportion of data fit by that mode (p_n) are shown. The fitting of mixtures was stopped when the probability exceeded 10%. *P* represents the probability that the data are better fit by a model containing the corresponding number of modes than by a model containing additional modes.

Table 2. *Fitting a mixture of von Mises distributions to mean heading vectors of flies in a no odor, plus wind environment*

Model	*gof* (U^2)	*P*	μ_1 (degrees)	*s* (degrees)	p_1	μ_2 (degrees)	*s* (degrees)	p_2
1VM	1.250	<0.01	–1.16±7.10	31.16	1.00	–	–	–
2VM	0.126	0.16	1.46±3.14	13.67	0.93	–145.29±36.20	39.96	0.07

Details as in Table 1.

upwind, flies manifested a centering response like the one described in honeybees by Srinivasan and colleagues (Fig. 3E) (Srinivasan et al., 1991). Because this response could have been influenced by visual orientation to the odor and fly releasing tubes, the analysis was restricted to the central 0.5 m of the tunnel.

Experiment 2: Object mediated orientation

The structure of the visual environment, especially the presence of conspicuous, high-contrast objects, influences the odor-mediated flight trajectories of *Drosophila* (Frye et al., 2003). We thus tested the relative strength of anemotaxis and target orientation in structuring flight trajectories by placing a black post, 1.27 cm in diameter and equal to the height of the tunnel, halfway along the tunnel's length and 6.35 cm from the nearest wall (Fig. 4). In the absence of wind, flies were strongly attracted to the post and 26% of fly transit, prior to landing, was within an imaginary cylinder of radius 14.5 cm centered on the post (Fig. 4A) (at which distance the post would subtend 5° of visual space). In the presence of a 0.4 m s^{-1} wind, however, the likelihood of cylinder occupancy was only 11% as the flies largely ignored the post while flying upwind (Fig. 4B).

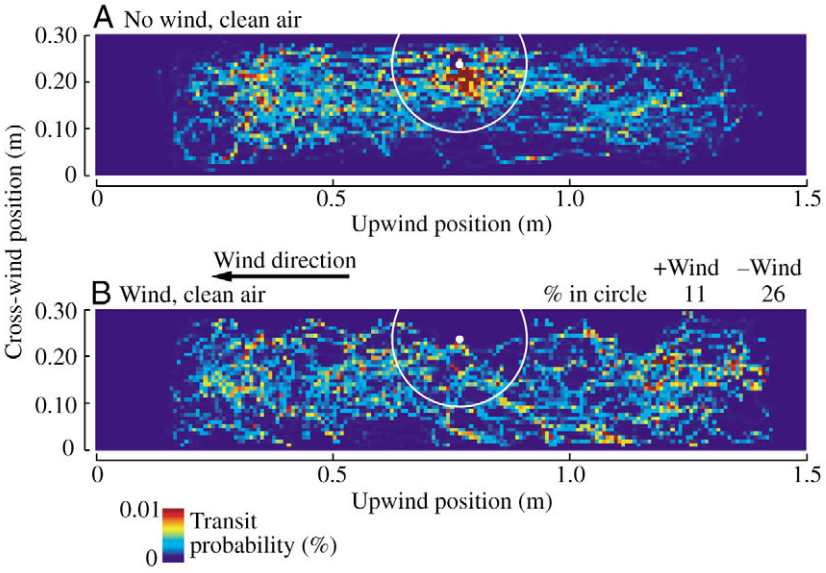

Fig. 4. Flies orient towards a conspicuous visual object, a black post (white dot), in the absence, but not in the presence of wind. Transit histograms, with flies viewed from above, in no wind (A, 67 flies) and in a 0.4 m s^{-1} wind (B, 39 flies). The white circle represents the distance from which the post would subtend 5° on a fly's retina. Without wind, 26% of total fly transit within the tunnel was located within the circle, but with wind this percentage dropped to 11%.

Experiment 3: Ribbon plume responses

Because of the highly reproducible flow conditions within the wind tunnel, we were able to estimate the location and size of the ribbon odor plume. This position was defined as a 1 cm diameter cylinder surrounding the measured path of a smoke plume that was introduced into the tunnel under identical flow conditions to those used to produce the ribbon odor plume, allowing us to estimate the time and place where the fly's trajectory intersected the odor plume. When exposed to a ribbon plume of banana odor in a 0.4 m s^{-1} wind, flies rapidly initiated flight and typically flew upwind, landing on either the odor release tube or the screen at the upwind end of the tunnel. The effects of plume contact on individual trajectories were often dramatic, but because of the variability of these flight responses, it would be misleading to present a single representative trajectory, and so instead, eight examples of plume oriented flight are shown in Fig. 5. At one extreme, many flies responded to plume contact by progressing almost directly upwind while increasing their

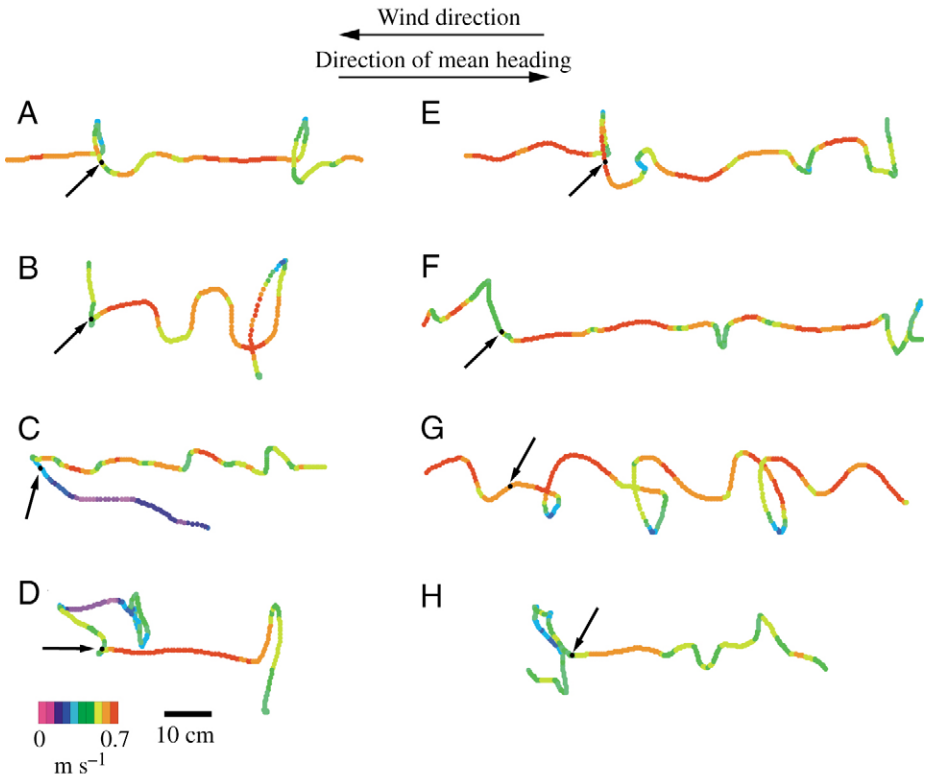

Fig. 5. (A–H) Eight examples of odor-mediated upwind flight with air speed encoded by color. The odor of fermented banana was presented to the flies in the form of a ribbon (1 cm diameter) plume. Flight trajectories, viewed from above, showed substantial variability following plume contact (plume contact indicated by arrow and black dot). Several features are often salient, however, including a shift from cross-wind to upwind flight as well as a fast upwind surge. Upwind progress is often interrupted by looping counterturns and casting flight directed across wind.

air speed (e.g. Fig. 5D). At the other extreme, some flies generated trajectories consisting of looping counterturns interspersed with periods of upwind progress (e.g. Fig. 5G). Between these two extremes, bouts of straight upwind flight often graded into more sinuous upwind flight (e.g. Fig. 5B,C,E). Despite the variability in responses to plume contact, several features were largely consistent such as the rapid shift from cross-wind to upwind flight, coupled with an increase in air speed following plume contact.

Because of the variability in overall trajectory shape, our analyses focused on short term changes in trajectory parameters associated with plume contact. Trajectories were thus partitioned into 'pre-contact' and 'post-contact' fragments. It is readily apparent, by plotting all of the post-contact fragments from each fly, that flies were able to follow the ribbon plume of banana odor to its source (Fig. 6A,B). In clean air, flies were much more evenly distributed throughout the tunnel, indicating that plume tracking was not a response to a narrow turbulent flow (Fig. 6C,D).

Analyzing pre-contact and post-contact fragments separately illustrates the substantial changes in flight trajectories that followed plume contact (Fig. 7). Prior to plume contact, flight was largely directed across wind. Taking the mean heading of entire trajectory fragments prior to plume contact however, tends to obscure this trend (since iterative tracks across wind result in a mean heading of 0°). Thus, a plot of total counts of instantaneous trajectory headings better illustrates the trimodal distribution of flight direction prior to plume contact, with modes at 0.00±18.16°, 84.77±49.35° and –80.89±41.79°, based on the fit of a mixture of three von Mises distributions (Fig. 7A). Following plume contact, headings were unimodally distributed around approximately 0° (Fig. 7B). Since these instantaneous headings are not independent of each other, they cannot be subjected to significance testing, and thus we calculated the mean pre- and post-contact trajectory headings for each fly based on all episodes of plume contact. A non-parametric test of the dispersion of these means indicates that flight prior to plume contact was significantly more highly dispersed around its mean of –4.98±47.21° than was flight following plume contact around its mean of 4.52±22.03° (N=138, U=5507, P<0.0001). Again testing trajectory means, flies increased their upwind velocity (pre-contact: 0.090±0.140 m s^{-1}, post-contact: 0.153±0.083 m s^{-1}) (t=4.53, d.f.=223.11, P<0.0001) as well as their total air speed (pre-contact: 0.55±0.11 m s^{-1}, post-contact: 0.59±0.08 m s^{-1}) (t=3.71, d.f.=250.94, P<0.001), while remaining closer to the plume (pre-contact: 0.053±0.024 m, post-contact:0.037±0.023 m), (t=5.46, d.f.=273.31, P<0.0001) (Fig. 7C).

To visualize the short-term effects of odor encounter on trajectory shape, pre-contact and post-contact fragments were translated and aligned at the point of plume contact (Fig. 8). Plotted in this way, the shift from cross-wind to upwind flight following plume contact is apparent (Fig. 8A). This effect was not attributable simply to entry into the center of the tunnel since in a clean air control, 'plume' contact, defined based on the location of a clean-air plume, did not result in any apparent systematic modification of the horizontal component of trajectory shape (Fig. 8B). Vertical displacement appeared less variable in the presence or absence of the plume suggesting

that flies may tend to maintain a relatively constant height in both conditions (Fig. 8A,B).

The immediate effects of plume contact on a variety of trajectory parameters were analyzed by plotting them as the time series averages of the first episode of plume contact recorded from each fly, aligned relative to the moment of plume contact (Fig. 9). Although plume contact appears to affect many parameters, the flies exhibit some of the same behaviors in response to the clean air control. An animal flying upwind can only encounter the plume if it flies vertically or cross-wind. An insect displacing laterally will eventually encounter the walls of the tunnel, eliciting a visually mediated collision avoidance response (Tammero and Dickinson, 2002), which would be likely to orient it upwind, given the anemotactic response shown in Fig. 2. Thus, to compare odor-mediated orientation and visual responses, we compared the changes in trajectories from the moment of plume contact (or its clean air equivalent) in flies flying in the presence and absence of odor. While many of the trajectory parameters changed with similar sign in both treatments, the timing of the responses was substantially advanced in the presence of odor. Because the maximal responses tended to occur within approximately 250 ms of odor contact, but within approximately 500 ms of entry into the no odor 'plume', we compared the changes from baseline values at those two time points (Table 3). In the presence of odor, flies reduced cross-wind velocity, increased upwind velocity and decreased heading significantly faster than in the clean-air control, resulting in a rapid 'upwind surge' within 250 ms, an interval corresponding to about 50 wingbeats. After 500 ms, however, there were no significant differences between the two treatments, suggesting that visual reflexes are sufficient to orient flies upwind following 'plume' contact. The upwind surge was coupled with a significant increase in air speed 250 ms after odor contact; not a surprising result if a fly heads more upwind in the absence of a compensatory decrease in ground speed. Indeed, changes in ground speed were not significantly different between the two treatments at either time point, reflecting the similar control exerted over this parameter under both conditions. Finally, vertical velocity was low prior to and following plume contact both in the presence and absence of odor, with no significant differences between the treatments, indicating stable altitude control. These results suggest that visually mediated responses to wall approach likely contributed to velocity modulation in the ribbon plume of banana odor as well as in the absence of odor.

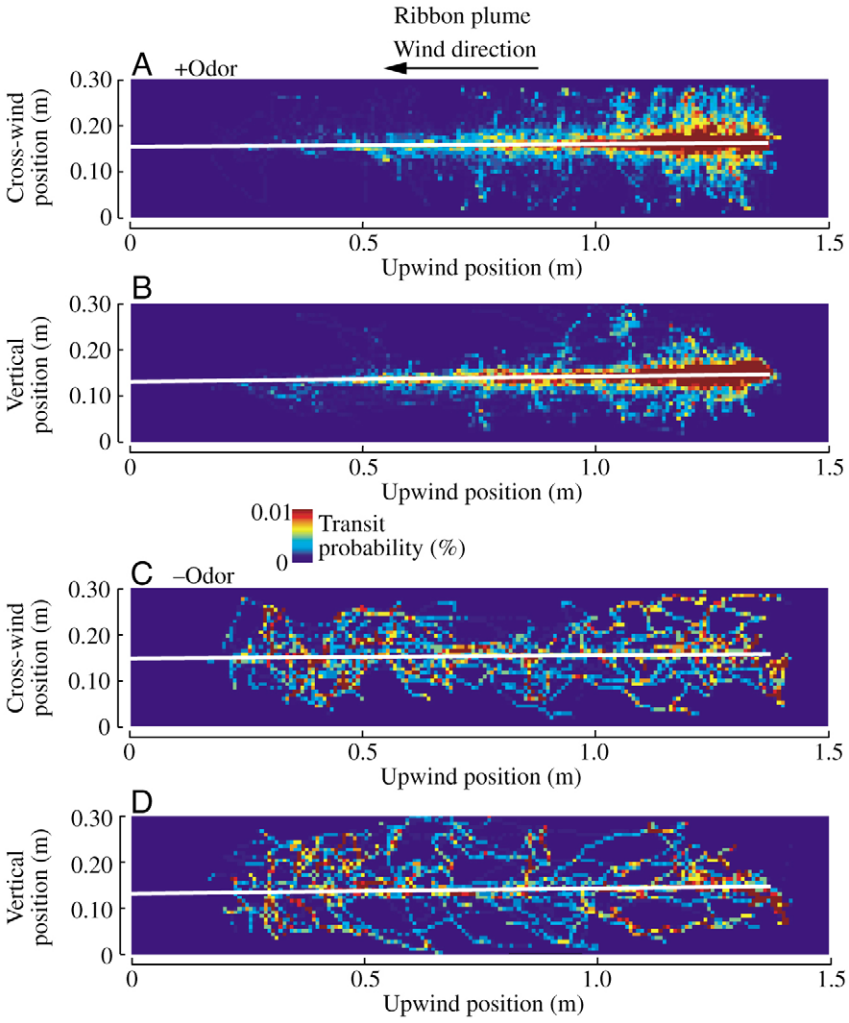

Fig. 6. Flies localize a ribbon plume of banana odor. Trajectories were partitioned into 'pre-contact' and 'post-contact' fragments. Transit histograms of post-contact flight indicate that flies localized and maintained close proximity to the plume (white bar) both in the horizontal (A) and vertical (B) dimensions (278 episodes of plume contact from 127 flies). In the absence of an odor plume, flies distributed much more uniformly throughout the tunnel (C and D, horizontal and vertical dimensions respectively, 51 episodes of 'plume contact' from 36 flies). Note that the plume did descend slightly along the tunnel's length and that the white bar accurately represents the approximate plume extent.

Experiment 4: Homogenous odor cloud responses

To determine whether the short-term surge response to plume contact was maintained in the face of constant stimulation, flies were tested in a homogeneous plume of banana odor that was introduced upstream of the tunnel's working section. While smoke visualization indicated that the plume was as fully mixed as possible within the constraints of our apparatus, it is possible that the tunnel contained some spatial variation of odor density. Nevertheless, in the face of the continuous stimulation, flies maintained the most

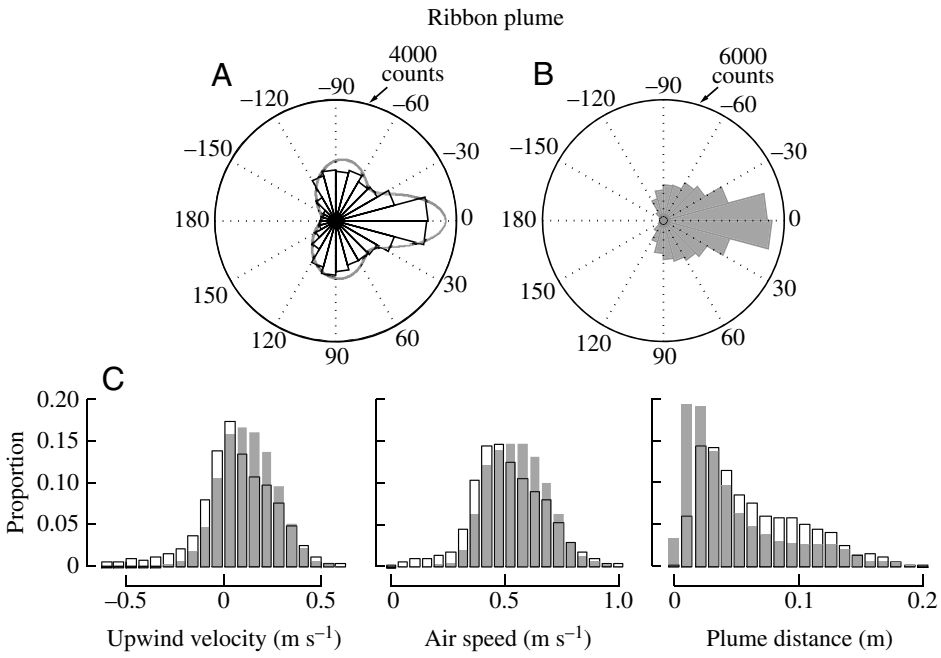

Fig. 7. Following plume contact, flies fly faster, straighter upwind. (A) Prior to plume contact, flight headings were distributed trimodally, with modes at 0.00±18.16°, 84.77±49.35° and –80.89±41.79°, based on the fit of a mixture of three von Mises distributions to the raw counts of instantaneous heading vectors. The shaded curve represents the trimodal model fit. (B) Following plume contact, flight was unimodally directed upwind (2.18±55.92°). For statistical analysis, mean pre- and post-contact headings were calculated for each fly. Mean pre-contact headings were significantly more dispersed than the corresponding post-contact means (N=138, U=5507, P<0.0001). (C) Proportions of the total counts of instantaneous trajectory values for upwind velocity, air speed and plume distance. Comparing trajectory means for each fly, upwind velocity increased following plume contact (t=4.53, d.f.=223.11, P<0.0001) as did air speed (t=3.71, d.f.=250.94, P<0.001), while the flies remained closer to the plume, (t=5.46, d.f.=273.31, P<0.0001) (pre-contact, empty bars; post-contact, filled bars, 138 flies).

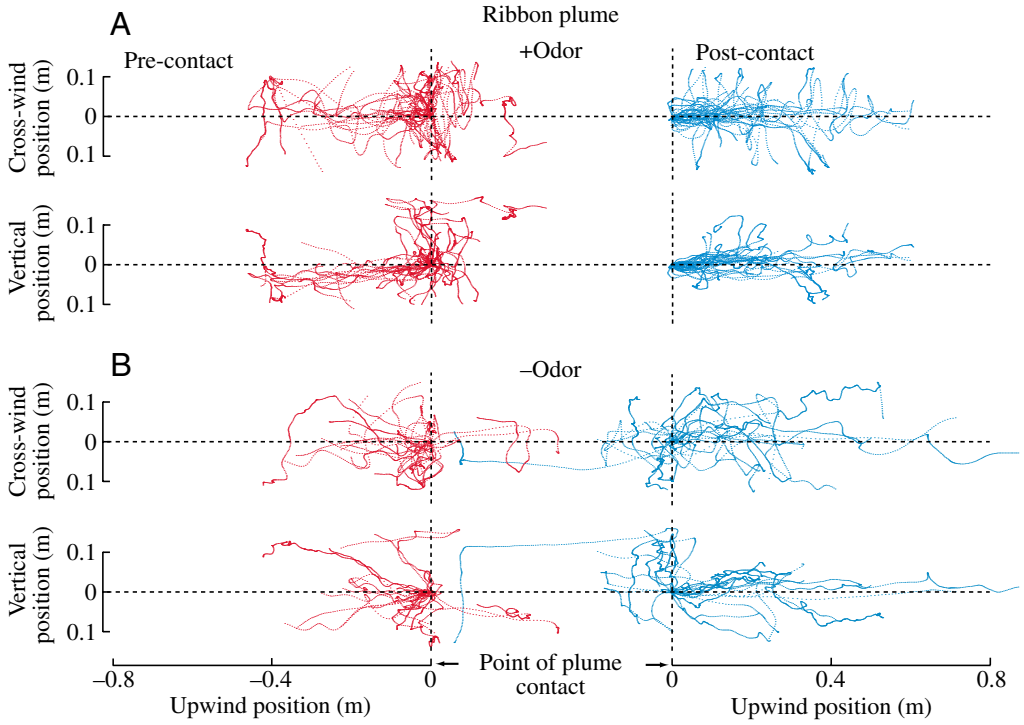

Fig. 8. Plume contact results in trajectories oriented along the plume line. 35 randomly selected episodes of plume contact were translated and aligned at the point corresponding to entrance into the plume cylinder in the banana odor ribbon plume and in a no odor control. (A) In the banana odor plume, pre-contact flight was largely directed across-wind whereas plume contact was followed by a shift towards upwind progress while maintaining close proximity to the plume-line with flies occasionally casting across wind. (B) In the absence of an odor plume, ‘plume’ contact lacked consistently similar effects on trajectory structure.

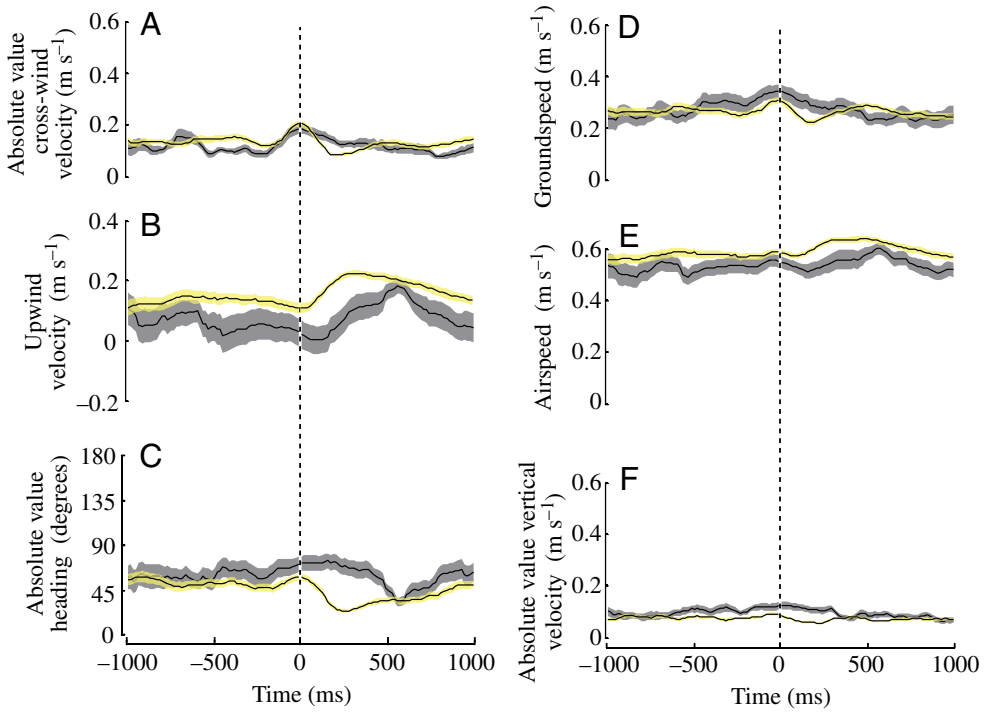

Fig. 9. Effects of contact with a ribbon plume of banana odor on kinematic parameters. The mean and standard error envelope are plotted for 1 s of flight prior to and following the first episode of plume contact in the banana odor ribbon plume (yellow error envelope, 124 flies) and in a no odor control (gray error envelope, 44 flies). Because not all trajectories consisted of at least 1 s of flight prior to and following plume contact, means and standard errors were calculated at all time points from all trajectories whose durations met or exceeded that threshold length.

consistently upwind flight headings that we observed under any condition (Fig. 10A,B), with significantly less dispersion around a mean of 0.49±21.98° than in a clean air control with mean –1.16±31.16° (N=80, U=2995, P<0.05). In addition to flying very straight upwind, flies increased their upwind velocities relative to a clean-air control (clean air: 0.053±0.105 m s^{-1}, homogeneous cloud: 0.131±0.120 m s^{-1}) (d.f.=171.84, t=4.57, P<0.0001) (Fig. 10C). Plotting several representative post-contact trajectories obtained in the homogeneous cloud, where 'contact' was again defined as it was in the clean-air case, illustrates the relative straightness of flight under this condition. (Fig. 11A,B). The strength of this effect is further illustrated by comparison with representative trajectories in the ribbon plume of banana odor showing the surges along the plume as described above, as well as bouts of flight directed primarily cross-wind (Fig. 11C). These cross-wind excursions are reminiscent of the casting behavior of moths (e.g. Kuenen and Baker, 1983; Marsh et al., 1978) and were less apparent in either the clean-air control or in the homogeneous cloud, suggesting a causal relationship between plume loss and casting.

Experiment 5: Pulsed plume responses

To assess the effects of plume loss on trajectory shape, flies were flown in a large diameter, pulsed banana plume. Pulses were generated for 1 s with a 50:50 duty cycle. To quantify casting behavior, a cast was defined as a change from upwind flight in which a trajectory showed six or more consecutive velocity vectors with heading angles whose absolute values were between 50° and 130°. Furthermore, we required that during a cast, a fly must move a minimum of 3 cm across wind. Although this definition is somewhat arbitrary, it effectively captures the qualitative difference in behavior that an observer can subjectively identify as a cast. In a separate series of trials,

Table 3. *Comparisons of changes in mean trajectory values from baseline in the narrow banana odor plume and a clean air control for six flight parameters at 250 and 500 ms following plume contact*

	250 ms			500 ms		
	d.f.	t	P	d.f.	t	P
Cross-wind velocity	86.64	2.54	<0.01	62.33	0.52	0.30
Upwind velocity	65.29	2.03	<0.05	75.48	1.29	0.10
Heading	58.47	3.55	<0.001	67.40	1.20	0.12
Ground speed	81.57	0.37	0.35	58.36	1.20	0.12
Air speed	60.10	1.93	<0.05	62.78	1.37	0.09
Vertical velocity	62.63	0.59	0.28	50.34	0.38	0.35

All values are calculated using one-tailed, heteroscedastic t-tests.

flies were flown in the same large diameter plume, but with a continuous rather than a pulsed odor structure. Our cast identification algorithm, in this case, searched for casts that initiated within the plume, allowing for the possibility that the cast itself would carry the animal outside of the plume. In all cases, our analysis was restricted to the first episode of plume contact for each fly.

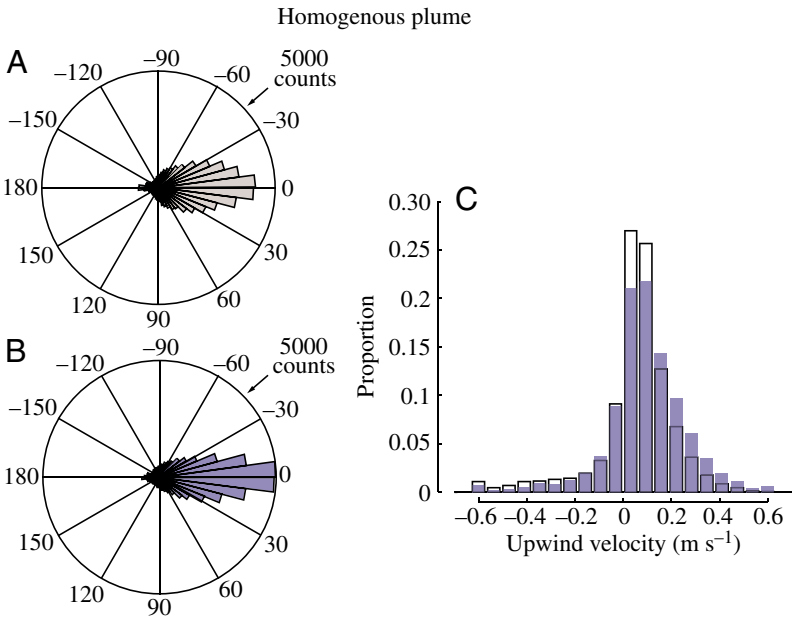

Fig. 10. In a homogeneous cloud, flight is directed almost completely upwind. (A) In a no odor control, wind polarized flight upwind (0.49±21.98°, 80 flies), but still resulted in greater dispersion of mean heading angles (N=80, U=2995, P<0.05) than in a homogeneous odor cloud (B, –1.16±31.16°, 94 flies). Note that raw heading counts are plotted, but only mean trajectory headings are analyzed statistically. Upwind flight was also significantly faster in the homogeneous cloud (d.f.=171.84, t=4.57, P<0.0001) (C, no odor, empty bars; homogeneous cloud, filled bars).

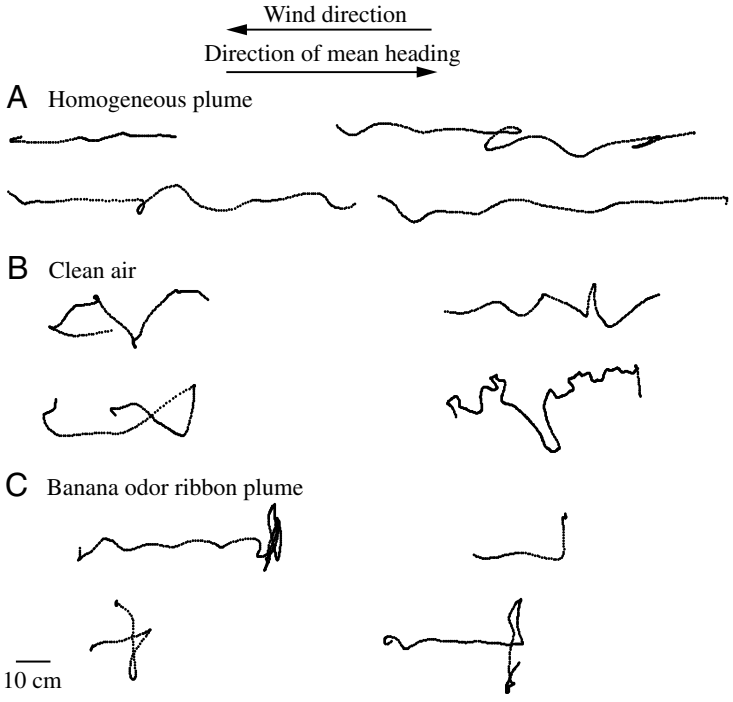

In the pulsed plume, flies frequently initiated casts following plume truncation, whereas in the continuous plume, trajectories tended to consist of sustained periods of upwind flight with few casts initiated while the fly was still in the plume (Fig. 12). Flies were significantly more likely to land on the plume source when flying towards a pulsed odor source (40%) than towards a pulsed no odor control (14%), (d.f.=1, χ^2=11.49, P<0.001), but landing probability was not significantly affected by plume structure in the presence of odor (46% landing probability in continuous plume, d.f.=1, χ^2=1.90, P<0.17).

The duration of plume contact could influence the likelihood of cast initiation, therefore we calculated the mean duration of contact prior to truncation of the pulsed plume (Fig. 13A). We then compared the probability of cast initiation following plume truncation to that following an equal duration spent in the continuous plume, a point of 'pseudo-plume truncation'. We required that casts initiate with a latency of at least one frame (16.7 ms) following truncation in order to ensure that the animals had exited the plume (Fig. 13B). Following actual or pseudo-plume truncation, many flies landed, or were lost by the visualization system, leading to a steady decline in the number of flies still 'eligible' to perform a cast. These pools were further reduced when flies in the pulsed plume encountered subsequent odor pulses, or when flies in the continuous plume flew out of its boundaries. The probability of cast initiation in each 50 ms bin following actual or pseudo-plume truncation was thus calculated as the number of flies that initiated casts within each bin divided by the number of flies in that bin that had not yet been excluded for any of the above reasons (Fig. 13D). Implementing this correction, flies were significantly more likely to initiate a cast in the first second following truncation of a pulsed plume than after an equivalent period in a

Fig. 11. Representative trajectories illustrate the differences between flight in a homogeneous cloud, clean air, and a banana odor ribbon plume. Four representative, 'post-contact,' trajectories are shown from (A) a homogeneous cloud, (B) clean air and (C) a banana odor ribbon plume. Flight in the homogeneous cloud often gave rise to very straight upwind trajectories compared to clean air. Trajectories in clean air headed generally upwind, while those in the banana odor ribbon plume were largely characterized by upwind flight interspersed with cross-wind casts.

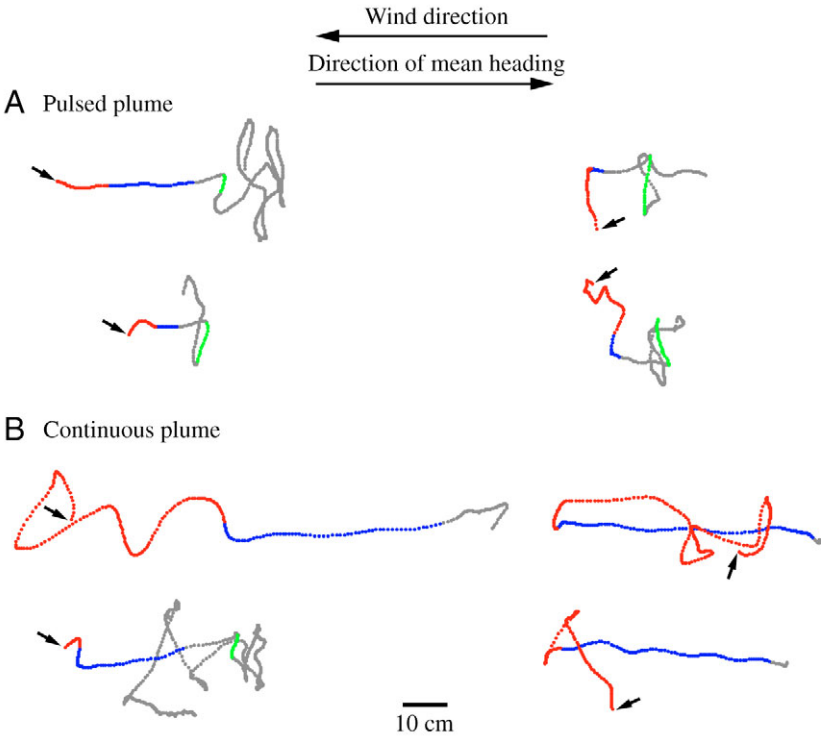

Fig. 12. Casting frequently follows plume truncation. (A) Four representative trajectories from the large diameter pulsed banana odor plume illustrate flight prior to plume contact (red), within the plume (blue), and following plume loss due to truncation (gray). The first cast, as defined by our cast identification algorithm, is plotted in green. (B) In the continuous large diameter plume, casting rarely initiated within the plume (color designations as above except that gray indicates plume loss due to flight out of the plume rather than plume truncation). Arrows indicate the initiation of fly tracking, but in some cases several points were excised from the beginning of the track in order to enhance the clarity of the trajectory.

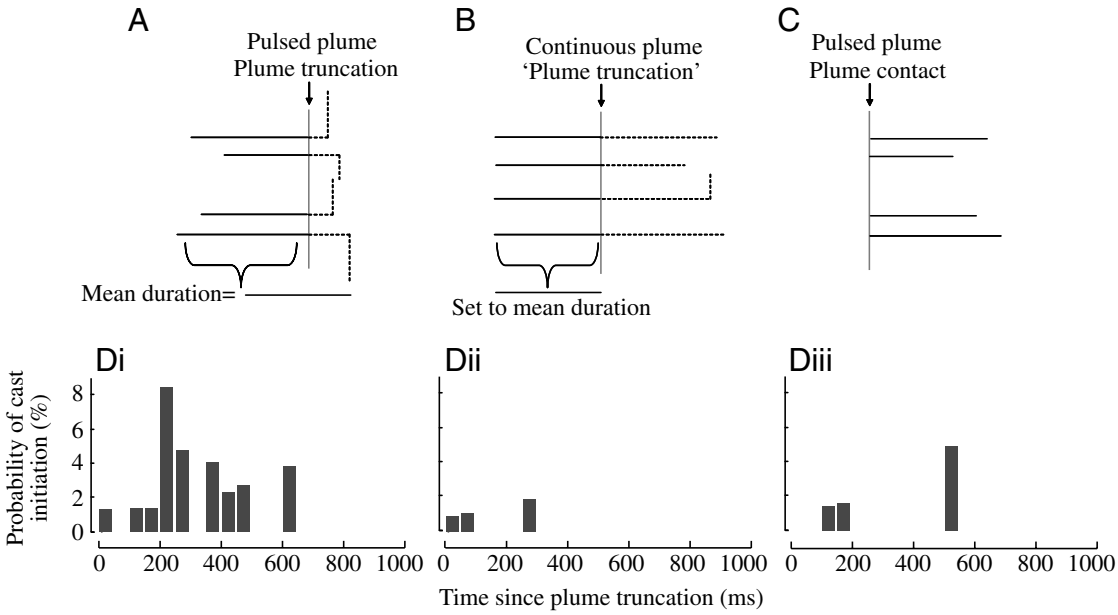

Fig. 13. Plume loss increases the probability of casting. (A) To test the effect of plume truncation on the probability of cast initiation, we calculated the mean duration of contact with a pulsed plume prior to truncation (383 ms). (B) The probability of casting following plume truncation was compared to that following 383 ms exposure to the continuous plume. The probability of cast initiation within each 50 ms bin following plume truncation, or 'pseudo-plume truncation', was then calculated as described in the text. Casting was significantly more likely following plume truncation than in the continuous plume (d.f.=1, χ^2=8.96, P<0.01), with 29.6% of flies initiating a cast within 1 s of plume truncation with a mean latency of 330±140 ms (Di). For flies in the pulsed plume, cast initiation was significantly more likely following plume truncation (Di) than following plume contact (Diii; d.f.=1, χ^2=6.66, P<0.01).

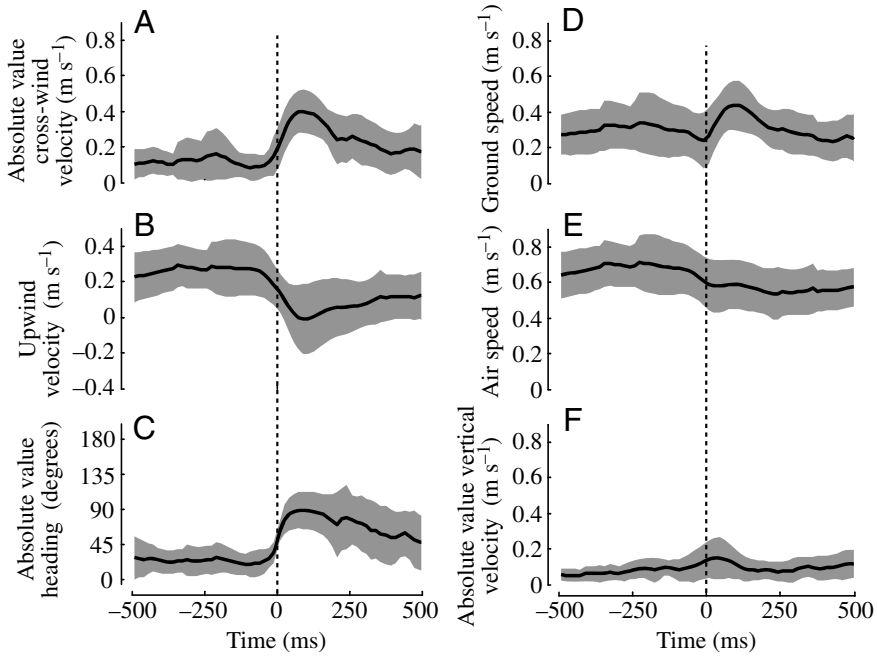

Fig. 14. (A–F) Effects of cast initiation on trajectory parameters. Kinematic parameters were aligned at the moment of cast initiation following plume loss due to truncation (mean and envelope of standard deviation are plotted). Casts manifested velocity profiles that were nearly the inverse of the plume contact response, with turns clearly initiating prior to reaching the 50° heading threshold necessary for the cast identification algorithm (C, 24 casts).

continuous plume (d.f.=1, χ^2=8.96, P<0.01). Following actual plume truncation, 17 flies (29.6%) casted within 1000 ms, with a mean latency of 330±140 ms to cast initiation. In the continuous plume, only three flies (3.6%) initiated a cast within 1000 ms following 'plume truncation'. We performed an analogous, within-fly analysis, for flies that experienced plume truncation in the pulsed plume. Here we compared cast initiation following plume contact (but while the fly still remained within the plume) to casting following truncation of that plume (Fig. 13A,C). We calculated the probability of cast initiation in each 50 ms bin following plume contact as the number of flies that initiated casts within each bin divided by the number of flies that had not yet suffered plume truncation. Casting probability following truncation was calculated as above. Following plume contact, three flies (7.7%) initiated casts within the plume, significantly fewer than initiated casts following plume truncation (d.f.=1, χ^2=6.66, P<0.01).

Restricting our analysis to flies that initiated casts following plume truncation, post-contact trajectories were partitioned and aligned at the moment of cast initiation. The effects of casting are largely the inverse of those elicited by plume contact (Fig. 14). Many of these effects are not surprising since they follow from the nature of the cast definition (that is, a modification of heading). It is also apparent that the initiation of those turns which will eventually result in crosswind flight (as judged from mean heading) precede cast initiation, as defined above, by approximately 40 ms on average (Fig. 14C).

Discussion

The results of this study indicate that food-deprived *D. melanogaster* readily initiate flight in the absence of an odor or even a wind stimulus. Furthermore, in the presence of a medium strength wind (0.4 m s^{-1}), this species is anemotactic (Fig. 3B). Previous studies on walking *D. melanogaster* had been inconclusive as to whether these flies are anemotactic in the absence of odor (Flugge, 1934; Johnston, 1982).

Theoretical arguments have suggested that flying insects should modulate their heading during olfactory search so as to maximize the likelihood of encountering an odor plume (Balkovsky and Shraiman, 2002; Dusenberry, 1989; Sabelis and Schippers, 1984). The present data indicate that in the absence of an olfactory stimulus, *D. melanogaster* tend to meander somewhat (Fig. 3B), while heading generally upwind, differing from two other *Drosophila* species whose flight headings do seem to fit the theoretical optimum whereby flight directed primarily across a steady wind maximizes the likelihood of plume contact (Zanen et al., 1994). Zanen and co-workers, however, studied flies in a wider (1 m) tunnel with a square footprint, and it is possible that the relatively narrow dimensions of our working section may have sufficiently inhibited cross-wind flight to mask such effects. On the other hand, flies did perform casts in our tunnel, indicating that the visual environment did not inhibit all cross-wind behavior.

Presumably, anemotaxis in *D. melanogaster* is accomplished *via* visual feedback, as in other insect species. Furthermore, the anemotactic response inhibits some visually mediated behaviors, including the otherwise robust attraction to conspicuous visual objects (Fig. 4). At the same time, anemotaxis does not universally suppress other mechanisms of visual guidance. For instance, while flying upwind, *D. melanogaster* seem to manifest a centering response reminiscent of that observed in honeybees flying along a narrow corridor (Fig. 3E) (Srinivasan et al., 1991). This suggests that flies, like bees, may balance the optic flow on both eyes in order to remain equidistant from the tunnel walls.

At the same time, flies were not limited to flight tracks that strictly followed the tunnel's midline and were somewhat dispersed across the width of the tunnel. Many flies did not head straight upwind, but instead repeatedly approached the walls, sometimes exhibiting saccadic maneuvers that are conspicuous in still air (Tammero and Dickinson, 2002). This suggests that expansion avoidance cues, generated by approach towards the tunnel walls, were also important in maintaining the flies' upwind heading, together with the anemotactic response.

In the presence of a ribbon plume of an attractive odor, pre-contact flight headings were trimodally distributed, with modal values at upwind and cross-wind headings (Fig. 7A). It seems likely that cross-wind directed 'pre-contact' flight may have largely consisted of casting responses to prior incidences of plume loss (Fig. 8A). Thus, whereas search trajectories did not seem to be directed across-wind in the absence of odor, following plume contact (and likely subsequent loss), flies initiated a qualitatively different sort of search behavior, mediated by casts, and which did frequently result in subsequent plume contact. These results suggest that *D. melanogaster* may indeed adhere to the theoretical prediction of cross-wind flight to increase the probability of plume encounter, but that expression of this strategy is dependent on prior plume contact.

In recent years, our understanding of olfactory-mediated search in insects has improved substantially. Recent experiments involving pulsed odor plumes have illustrated the degree to which flight trajectories may be shaped by responses to instantaneous stimulus experience (Mafra-Neto and Cardé, 1994; Vickers and Baker, 1994). This finding makes it realistic to imagine that a comprehensive understanding of short-term stimulus responses could be adequate to explain the emergent behavior.

Baker has articulated an elegant model for olfactory flight control (Baker, 1990), whereby a phasically modulated response to plume contact generates an upwind surge and a separate, tonic response, activates an internal counterturn generating mechanism. Suppression of the tonic mechanism by the phasic one in response to a pulsed plume of the appropriate frequency could result in an iterated series of upwind surges, fusing to form straight upwind flight. While it nicely explains the results of many experiments on moths, the applicability of Baker's model to flight in other insect orders is still unclear. In this study, we found that *D. melanogaster*, like many moth species, seem to surge upwind following plume contact. This is accomplished by turning into the wind while increasing air speed. It is important to note that animals in a clean-air control also turn upwind following 'plume contact', though this response is significantly delayed (Fig. 9). The most parsimonious explanation for this surge in the absence of odor is that the response is caused by a visually mediated collision avoidance reflex elicited by approach to the tunnel walls coupled with the anemotactic response. Visual responses are thus likely to be involved in plume-mediated trajectory modifications, though it is difficult to disentangle those here due to the spatial dimensions of the tunnel. Similar visual reflexes may play a role in many wind tunnel studies of olfactory behavior, a problem compounded by differences in tunnel geometry between studies.

The Baker model predicts that in the face of constant stimulation, the tonic, counterturn generating pathway should be engaged, and that indeed is what occurs in *Adoxophyes orana* (Kennedy et al., 1980) and *Grapholita molesta* (Willis and Baker, 1984), where moths cast widely in homogeneous plumes. It thus seems somewhat surprising that at very high pulse frequencies, where the resulting plume may approach contiguity (Vickers and Baker, 1992), comparatively straight upwind flight occurs in at least two species of moths, *Cadra cautella* and *Heliothis virescens* (Mafra-Neto and Cardé, 1994; Vickers and Baker, 1994). One might have expected that casting would be elicited as the pulsed plume approximated a continuous one. Recent work (Justus and Cardé, 2002) has indicated that one of those species, *C. cautella*, may indeed fly upwind in the presence of a homogeneous plume, differing substantially from *A. orana* (Kennedy et al., 1980), *G. molesta* (Willis and Baker, 1984) and *P. gossypiella* (Justus and Cardé, 2002). It is somewhat difficult, however, to compare the behavior in the homogeneous plume to that in pulsed plume experiments since overall trajectory vectors were presented rather than instantaneous heading histograms.

D. melanogaster, as suggested by the anecdotal studies of Wright and colleagues, respond in an apparently qualitatively different fashion from several moth species (besides, perhaps, *C. cautella* as described above), when exposed to a homogeneous odor plume (Kellogg et al., 1962; Wright, 1964). Under that condition, *D. melanogaster* consistently exhibited the straightest upwind trajectories that we observed in any treatment, and thus seem to depart from the Baker model for moth flight in that flies' upwind response to an attractive odor does not adapt to constant stimulation in the short term. This finding is consistent with tethered flight experiments in which *D. melanogaster* increases wing beat frequency and amplitude in response to ongoing stimulation (Frye and Dickinson, 2004a) (S.A.B., unpublished observations).

D. melanogaster also sometimes cast across-wind when exposed to the banana odor ribbon plume, and our plume truncation results indicate a causal relationship between plume loss and cast initiation. Cast latencies are somewhat variable, with a mean value near 290 ms. A fairly wide range for this parameter has been reported in the moth literature, with a shift to cross-wind flight within 150–220 ms in *G. molesta* (Baker and Haynes, 1987), 490 ms in *Manduca sexta* (Willis and Arbas, 1991), 710 ms in *C. cautella* (Mafra-Neto and Cardé, 1996) or about 1 s in *Lymantria dispar* (Kuenen and Cardé, 1994). Kellogg et al. even suggested a value of about 100 ms for *D. melanogaster*, based on their anecdotal results (Kellogg et al., 1962). Despite this variability in the timing of initiation, it is interesting that this flight maneuver is shared with the phylogenetically distant Lepidoptera and implies perhaps that the problem of olfactory search is sufficiently universal to often rely on the same search algorithms. This algorithmic

similarity may represent a homology in neural circuitry or it may indicate convergence on a relatively universal and optimal strategy for odor localization.

The behavior of *D. melanogaster* in the homogeneous cloud suggests that the upwind response is tonically rather than phasically activated, though it initiates rapidly in response to plume contact. Further, although *D. melanogaster* do perform casting maneuvers following plume loss, it is impossible to conclude from these data whether casts are generated by an internal mechanism, as they are in many moth species, or whether they represent a phasic response to plume loss. If these turns are the output of a tonically active counterturn generator, similar to the one proposed by Baker, then the results suggest that a fast activating tonic upwind odor response is capable of suppressing the counterturn generator in *D. melanogaster*. If, however, cast initiation in *D. melanogaster* is strictly a phasic response to plume loss, it may simply never be triggered in the homogeneous cloud. Regardless of the underlying mechanism, however, it is important to note that the precise architecture of casts is likely to also be shaped by the collision avoidance response and thus wind tunnel design.

The present results are consistent with those of previous tethered flight experiments on visual and olfactory responses in *D. melanogaster* (Frye and Dickinson, 2004a; Frye and Dickinson, 2004b). In those studies, flies responded to stimulation with an attractive odor by increasing wing beat frequency and amplitude. Because the relationship between force production and wing kinematics is complex, it was impossible to infer the precise effects of those kinematic changes on flight forces. In this study, however, we can relate olfactory stimulation to air speed, an index of force production. Airspeed increases following plume contact have a time course similar to that of the wing responses observed by Frye and Dickinson (Frye and Dickinson, 2004a; Frye and Dickinson, 2004b). Similarly, the tethered flight responses do not decay over a 5 s stimulation period, suggesting that the increase in force production does not adapt quickly to sustained stimulation, in strong agreement with the results reported here in the homogeneous cloud.

An additional finding (Frye and Dickinson, 2004a) was that visually evoked steering reflexes were almost completely independent of the olfactory response in tethered flight. Further work has revealed, however, that flies stabilize large-field image motion better in the presence of an attractive odor (Frye and Dickinson, 2004b), and this result is consistent with the very straight trajectories that we observed in the homogeneous cloud. It thus seems as though some, but not all, visual responses are affected by olfactory stimulation. This makes it difficult to assess the degree to which upwind plume tracking in *D. melanogaster* might consist simply of thrust responses to olfactory stimulation superimposed on a visually controlled behavior, or whether the behavior results instead from modulation of visual responses by olfactory stimuli. A likely example of such modulation is the occurrence of casts, an olfactory triggered behavior that is unlikely to have been predicted from models of flight control dominated by visually mediated expansion avoidance or centering responses. Though ‘spontaneous’ saccades do sometimes occur in a tethered flight arena in the absence of odor, and thus could conceivably be responsible for cast initiation, it would be difficult to explain iterated large magnitude turns and cross-wind flight strictly as the result of the visually based flight control mechanisms mentioned above.

Despite the general accord between tethered and free-flight behavior, the results in the two paradigms may not be entirely consistent. In the case of the response to plume loss, one might have expected that the cessation of olfactory stimulation in tethered flight would result in a fictive turn, corresponding to cast initiation. However, this does not seem to be the case, as odor pulse termination does not tend to increase turning rate (Frye and Dickinson, 2004a). This may be a result of the relatively long odor pulses used in those experiments, or it may be related to the deficiency of mechanosensory cues in tethered flight, a question that we are currently pursuing.

It is clear that there is substantial variability in plume-mediated flight trajectories, even in the short-term responses to plume contact. One of the chief limitations of all wind tunnel studies is the lack of control over instantaneous stimulus conditions. Not only is the olfactory stimulus invisible, but the exact conditions under which stimulus encounter occurs, both in terms of the precise stimulus history of the animal, as well as its current stimulus environment, are extremely difficult to ascertain. This limitation of the paradigm is also one of its strengths in that it allows for a relatively naturalistic environment in which to test olfactory and visual responses. In as much as odor-mediated flight trajectories may emerge from near-instantaneous responses to short term stimulus conditions, it should be possible to explain *D. melanogaster* flight in terms of the dynamics of the response to odor encounter and loss. This study has begun that process by documenting the short-term response to plume encounter and loss, and the long-term response to constant odor stimulation. The challenge now is to more precisely characterize the responses to odor contact and loss, eventually permitting the construction of a behavioral model capable of explaining the variability in odor-mediated free-flight trajectories. The most obvious way to accomplish this is by varying pulse presentation schedules in a controlled manner in a tethered flight arena; this is an avenue of research that we are currently pursuing.

The authors wish to thank Titus Neumann for his assistance with the fly visualization system, Andrew Straw for help in programming the pulse generating system and Dan Rizzuto for his implementation of the non-parametric test for common mean dispersion. The manuscript also benefited greatly from the comments of two anonymous reviewers. This work was supported by an NSF predoctoral fellowship to S.A.B. and by grants from the Packard Foundation and the Institute for Collaborative Biotechnologies through grant DAAD19-03-D-0004 from the Army Research Office.

References

Baker, T. C. (1990). Upwind flight and casting flight: complimentary phasic and tonic systems used for location of sex pheromone sources by male moths. In *International Symposium on Olfaction and Taste* X (ed. K. B. Doving), pp. 18-25. Oslo: Graphic Communications Systems.

Baker, T. C. and Haynes, K. F. (1987). Manoeuvres used by flying male oriental fruit moths to relocate a sex pheromone in an experimentally shifted wind-field. *Physiol. Entomol.* **12**, 263-279.

Baker, T. C., Willis, M. A., Haynes, K. F. and Phelan, P. L. (1985). A pulsed cloud of sex pheromone elicits upwind flight in male moths. *Physiol. Entomol.* **10**, 257-265.

Balkovsky, E. and Shraiman, B. I. (2002). Olfactory search at high Reynolds number. *Proc. Natl. Acad. Sci. USA* **99**, 12589-12593.

Batschelet, E. B. (1981). *Circular Statistics in Biology*. New York: Academic Press.

Cardé, R. T. and Minks, A. K. (1997). *Insect Pheromone Research: New Directions*. New York: Chapman & Hall.

Carson, H. L. and Heed, W. B. (1986). Methods of collecting *Drosophila*. In *The Genetics and Biology of Drosophila*. Vol. 3e (ed. M. Ashburner, H. L. Carson and J. N. Thompson), pp. 1-28. New York: Academic Press.

David, C. T. (1979a). Height control by free-flying *Drosophila*. *Physiol. Entomol.* **4**, 209-216.

David, C. T. (1979b). Optomotor control of speed and height by free-flying *Drosophila*. *J. Exp. Biol.* **82**, 389-392.

David, C. T. (1982). Compensation for height in the control of ground speed by *Drosophila* in a new, 'barber's pole' wind tunnel. *J. Comp. Physiol. A* **147**, 485-493.

Dusenberry, D. B. (1989). Optimal search direction for an animal flying or swimming in a wind or current. *J. Chem. Ecol.* **15**, 2511-2519.

Fisher, N. I. (1993). *Statistical Analysis of Circular Data*. Cambridge: Cambridge University Press.

Flugge, C. (1934). Geruchliche raumorientierung von *Drosophila melanogaster*. *Z. Vergl. Physiol.* **20**, 463-500.

Fry, S., Bichsel, M., Muller, P. and Robert, D. (2000). Tracking of flying insects using pan-tilt cameras. *J. Neurosci. Methods* **101**, 59-67.

Frye, M. A. and Dickinson, M. H. (2004a). Motor output reflects the linear superposition of visual and olfactory inputs in *Drosophila*. *J. Exp. Biol.* **207**, 123-131.

Frye, M. A. and Dickinson, M. H. (2004b). Visuo-motor responses to attractive odorants during tethered flight in *Drosophila*. In *7th Congress of the International Society for Neuroethology*, Abstract PO103. Nyborg, Denmark: University of Southern Denmark.

Frye, M. A., Tarsitano, M. and Dickinson, M. H. (2003). Odor localization requires visual feedback during free flight in *Drosophila melanogaster*. *J. Exp. Biol.* **206**, 843-855.

Geier, M., Bosch, O. J. and Boeck, J. (1999). Influence of odour plume structure on upwind flight of mosquitoes towards hosts. *J. Exp. Biol.* **202**, 1639-1648.

Johnston, J. S. (1982). Genetic variation for anemotaxis (wind-directed movement) in laboratory and wild-caught populations of *Drosophila*. *Behav. Genet.* **12**, 281-293.

Justus, K. A. and Cardé, R. T. (2002). Flight behaviour of two moths, *Cadra cautella* and *Pectinophora gossypiella*, in homogeneous clouds of pheromone. *Physiol. Entomol.* **27**, 67-75.

Kellogg, F. E., Frizel, D. E. and Wright, R. H. (1962). The olfactory guidance of flying insects. IV. *Drosophila*. *Can. Entomol.* **94**, 884-888.

Kennedy, J. S. (1940). The visual responses of flying mosquitoes. *Proc. Zool. Soc. Lond. Ser. A* **109**, 221-242.

Kennedy, J. S. (1983). Zigzagging and casting as a programmed response to wind-borne odour: a review. *Physiol. Entomol.* **8**, 109-120.

Kennedy, J. S. and Marsh, D. (1974). Pheromone-regulated anemotaxis in flying moths. *Science* **184**, 999-1001.

Kennedy, J. S., Ludlow, A. R. and Sanders, C. J. (1980). Guidance system used in moth sex attraction. *Nature* **288**, 475-477.

Kennedy, J. S., Ludlow, A. R. and Sanders, C. J. (1981). Guidance of flying male moths by wind-borne sex pheromone. *Physiol. Entomol.* **6**, 395-412.

Kuenen, L. P. S. and Baker, T. C. (1983). A non-anemotactic mechanism used in pheromone source location by flying moths. *Physiol. Entomol.* **8**, 277-289.

Kuenen, L. P. S. and Cardé, R. T. (1994). Strategies for recontacting a lost pheromone plume: casting and upwind flight in the male gypsy moth. *Physiol. Entomol.* **19**, 15-29.

Mafra-Neto, A. and Cardé, R. T. (1994). Fine-scale structure of pheromone plumes modulates upwind orientation of flying moths. *Nature* **369**, 142-144.

Mafra-Neto, A. and Cardé, R. T. (1996). Dissection of the pheromone-modulated flight of moths using single-pulse response as a template. *Experientia* **52**, 373-379.

Marsh, D., Kennedy, J. S. and Ludlow, A. R. (1978). An analysis of anemotactic zigzagging flight in male moths stimulated by pheromone. *Physiol. Entomol.* **3**, 221-240.

Sabelis, M. W. and Schippers, P. (1984). Variable wind directions and anemotactic strategies of searching for an odour plume. *Oecologia* **63**, 225-228.

Srinivasan, M., Lehrer, M., Kirchner, W. H. and Zhang, S. W. (1991). Range perception through apparent image speed in freely flying honeybees. *Vis. Neurosci.* **6**, 519-535.

Tammero, L. F. and Dickinson, M. H. (2002). The influence of visual landscape on the free flight behavior of the fruit fly *Drosophila melanogaster*. *J. Exp. Biol.* **205**, 327-343.

Vickers, N. J. and Baker, T. C. (1992). Male *Heliothis virescens* maintain upwind flight in response to experimentally pulsed filaments of their sex pheromone (Lepidoptera: Noctuidae). *J. Insect Behav.* **5**, 669-687.

Vickers, N. J. and Baker, T. C. (1994). Reiterative responses to single strands of odor promote sustained upwind flight and odor source location by moths. *Proc. Natl. Acad. Sci. USA* **91**, 5756-5760.

Willis, M. A. and Arbas, E. A. (1991). Odor-modulated upwind flight of the sphinx moth, *Manduca sexta* L. *J. Comp. Physiol. A* **169**, 427-440.

Willis, M. A. and Baker, T. C. (1984). Effects of intermittent and continuous pheromone stimulation on the flight behavior of the oriental fruit moth, *Grapholita molesta*. *Physiol. Entomol.* **9**, 341-358.

Wright, R. H. (1964). *The Science of Smell*. London: G. Allen & Unwin.

Zanen, P. O., Sabelis, M. W., Buonaccorsi, J. P. and Cardé, R. T. (1994). Search strategies of fruit flies in steady and shifting winds in the absence of food odours. *Physiol. Entomol.* **19**, 335-341.